Spin probe interaction and mobility in confined cyclohexane: effects of pore size and pore surface composition of silica gel matrices

M. Lukešová, H. Švajdlenková, Daniel Reuter, S. Valić, Alois Loidl, J. Bartoš

Angaben zur Veröffentlichung / Publication details:

Lukešová, M., H. Švajdlenková, Daniel Reuter, S. Valić, Alois Loidl, and J. Bartoš. 2019. "Spin probe interaction and mobility in confined cyclohexane: effects of pore size and pore surface composition of silica gel matrices." *Chemical Physics Letters* 735: 136756. https://doi.org/10.1016/j.cplett.2019.136756.

Spin probe interaction and mobility in confined *cyclohexane*: Effects of pore size and pore surface composition of *silica gel* matrices

M. Lukešová[a,1], H. Švajdlenková[a], D. Reuter[b], S. Valić[c,d], A. Loidl[b], J. Bartoš[a,*]

[a] *Polymer Institute of SAS, Dúbravská cesta 9, SK-845 41 Bratislava, Slovakia*
[b] *Experimental Physics V, CECM, University of Augsburg, D-861 35 Augsburg, Germany*
[c] *Ruđer Bošković Institute, Bijenička cesta 54, HR-10000 Zagreb, Croatia*
[d] *Faculty of Medicine, University of Rijeka, Braće Branchetta 20, HR-51000 Rijeka, Croatia*

A B S T R A C T

The spectral behavior of the spin probe *TEMPO* in the bulk *cyclohexane* (*CHX*) and its confined states in a series of *silica gels* (*SG*) using ESR is reported. The spectral parameter $A_{zz'}$ and the characteristic ESR temperature T_{50G} of slow to fast regime transition of *TEMPO* change dramatically in the virgin *SG-SIL*'s compared to the bulk *CHX* sligtly depending on the pore size. These observations result from the interrelation between the mutual interaction of the *TEMPO* with the *SG*'s and the altered phase behavior of the *CHX* from DSC. This is supported by the modified (silanized) *SG matrices*.

1. Introduction

The topic of bulk vs. confined organic *materials* is usually studied by a variety of classic experimental techniques. Thermodynamic, structural and dynamic behaviors of various *organic media* are investigated by means of calorimetry, diffraction and scattering, resonance as well as relaxation spectroscopies determining characteristic material properties, such as enthalpy, static and dynamic density fluctuations, electric and magnetic dipoles, etc - see general and special reviews [1–8]. Significant changes in various physical properties are often observed which are related to phase transitions and eventually, to a formation of new phase(s) induced in confined organic *medium* (*filler*) by spatial restriction or/and by wall surface of *confining* inorganic *matrix* (*confiner*) [1–4] as well as to complex dynamic properties [5–8]. The overall confinement effect is considered to be a result of the complex mutual interplay of the two main factors: (i) geometric restricting effects of the pores on the *medium* in a given *matrix* and (ii) the mutual interaction effects of the *medium* with the pore surface wall of the *matrix* [1–8].

On the other hand, non-standard experimental techniques using various *molecular* and even *atomic*-sized *extrinsic probes*, such as *stable free radicals* or *positronium,* respectively, via electron spin resonance (ESR) [9–18] or positron annihilation lifetime spectroscopy (PALS) [19–22] are utilized to characterize the bulk state [9–13] and especially, the confined organic *media* [14–18,19–22] in essentially smaller extent. One of the promising microscopic probes are the so-called *spin probes* of nitroxide type, e.g., *2,2,6,6-tetramethyl-piperidinyl-1-oxy* (*TEMPO*) via ESR [14,15,23]. Advantages of *nitroxide probes* are their simple ESR spectra and their sensitivity to interaction with surroundings and to their reorientation dynamics in a given *medium* or/and *matrix*. However, in comparison to the standard techniques, one *additional* parameter comes into the characterization problem. Although the *spin probe* concentration in a given *organic medium* is very small, typically of 1-5x10^{-4} M, and the related *medium* perturbation by *extrinsic probe* seems to be apparently negligible, it is necessary to address the

* Corresponding author.
E-mail address: Jozef.Bartos@savba.sk (J. Bartoš).
[1] Present address: Institute of Macromolecular Chemistry, Czech Academy of Sciences, Heyrovského nám. 2, 162 06 Prague 6, Czech Republic.

special aspect of potential interparticle interaction between this incorporated *probe* and the confined organic *filler* versus that between *the probe* and the pore wall of *the* confining inorganic *confiner*.

Recently, a potential role of this interaction aspect together with its impact into reorientation dynamics was suggested for *apolar* linear hydrocarbon, namely, *n-hexadecane* (*n-HXD*) in a series of *polar* unmodified *silica gel* (*SG*) *matrices* as probed by *polar spin probe TEMPO* [14]. The spectral behavior of *TEMPO* was charaterized via the extrema line separation of the triplet signal, $2A_{zz'}$ [9,11,13], as a function of temperature *T* from 100 K up to 360 K. The most pronounced features in the quasi-sigmoidal $2A_{zz'}$ vs. *T* plot are i) the relatively high $2A_{zz'}$ value in the immobilized state around 80 Gauss and ii) a transition from slow to fast motion regime at the convential characteristic ESR temperature, T_{50G}, i.e., the temperature at which $2A_{zz'} = 50$ Gauss corresponding to the correlation time of the *spin probe* of a few nanoseconds [11,13]. It was found that the *TEMPO* dynamics is very strongly slowed down with respect to that in the bulk *medium* because of the dramatic increase of the T_{50G}(bulk) value by about 100 K. Moreover, in a set of *three* unmodified *SG-SIL matrices* with the mean pore size ranging from 300 Å through 100 Å down to 60 Å, the T_{50G} value increases moderately within ca. 15 K. These findings were interpreted as a result of the preferential interaction of the *polar TEMPO* molecule with the *polar silanol* groups at the pore surface of the unmodified *SG-SIL matrices*. This explanation is supported by (i) the empirical fact that the high $2A_{zz'}$ value of the *TEMPO* in the fast regime in the confined state of all the unmodified *SG matrices* reaches about 40 Gauss which is comparable to the reported one of 39 Gauss for the similar nitroxide-type *spin probe di-terc-butyl nitroxide* (*DTBN*) adsorbed in bare *silica gel* at RT [24] and by (ii) theoretical results from quantum-mechanical calculations of the $A_{zz'}$ parameter for the isolated and the attached (bound) *nitroxide radical* to …H—O group [25]. Consequently, the following natural question arises: Whether and under what conditions ESR is able to reflect *correctly* the altered structural-dynamic state of the confined *organics* of a given *apolar* structural type in various kinds of SiO_2-based *matrices* differing in their surface structure, i.e., in unmodified vs. modified *ones* in comparison with the reference bulk state of the *organics* ?

Cyclohexane (*CHX*) was often used as a typical representative of *apolar* crystallizing organic *media* with the globular molecules in the confinement studies by standard thermodynamic, structural and dynamic techniques, such as DSC [26–33], x- and n-DIFF [34,35] and NMR [36–39]. Thus, *Jackson* and *McKenna* were the first to demonstrate systematically using DSC a strong effect of the spatial restriction on the main *solid*-to-*liquid* phase transition at T_m of various *apolar organics*, including *CHX*, in a series of irregular *control porous glasses* (*CPG*) *matrices* modified by silalyzation to make their pore surface more hydrophobic with consequently better wetting to *apolar media* [26]. Later, Malhotra et al. showed using DSC that also the *solid*-to-*solid* (plastic crystal) phase transition temperature, T_{ss}, of *CHX* caused by small-scale reorientation of the quasi-spherical molecule is altered by confinement in a series of irregular modified *silica gel* (*SG*) *matrices* after the dehydratation and dehydroxylation treatment [27,28]. Next, *the latter authors* found out that both the freezing T_f and melting T_m temperatures of *CHX* in the three modified *silica gels* exhibit the non-monotonous course as a function the alkyl-type modifier substituent's length in the surface wall structure [29]. Finally, *CHX* was also investigated in various regular *matrices*, such as *silicon* [31] and unmodified (virgin) *MCM-41* and *SBA-15* [32]. Dosseh et al. [33] used the three regular unmodified *SBA-15 matrices* and reported the *apparently very strong* difference in the reduction of the melting temperature in comparison with the irregular modified *CPG* [26] and *SG* [27] *ones* ascribed to the difference in their surface chemistry. On the other hand, extrinsic *probe* studies of this model *apolar cyclic* aliphatic *compound* in some confined states are still missing.

Recently, we have investigated *CHX* in the bulk state by a combination of two extrinsic *probe* techniques using ESR and PALS [40]. It was found that T_{50G} correlates with the *solid*- to-*solid* phase transition at T_{ss}(bulk) lying deep in the *solid* state about ca. 95 K below the *solid*-to-*liquid* (melting) point T_m(bulk). This agreement indicates that the reorientation of the *TEMPO* is closely related to the reorientation motion of the *CHX* molecules being responsible for the T_{ss}(bulk) transition. In the light of several afore-mentioned standard characterization studies of confined *CHX* it is of interest to reveal the information potential of ESR by addressing the following two important apects, namely, molecular shape and mutual interaction aspect in the three-*component system* with respect to the two-*component system* in standard techniques. To solve this question the *apolar cyclohexane* (*CHX*) *medium* formed by the quasi-spherical molecules which embedded in a series of both unmodified and two differently modified *silica gel* (*SG*) *matrices* is investigated by ESR and DSC techniques.

2. Experimental

2.1. Materials

Cyclohexane (*CHX*) with the purity of 99.5% from Sigma–Aldrich, Inc., Germany was used.

A series of unmodified (virgin) and modified (silanized) *silica gels* KROMASIL® consisting of spherical particles with outer diameters of 10 μm were obtained from Eka Chemicals, Bohus, Sweden. The pore diameters D_{pore} in the virgin *silica gels* named as *SG60-SIL*, *SG100-SIL* and *SG300-SIL* were determined by *the supplier* to be 60, 100 and 300 Å. The virgin *silica gel SG100* matrix was chemically bonded by *dimethylalkylsilyl* groups of various length and the modified *SG100 matrices* were designed as *SG100-C4* (*dimethylbutylsilyl*) and *SG100-C18* (*dimethyloctadecylsilyl*). According to *the supplier* the total surface concentration of *silanol* groups is 8 μmol/m^2 in the original *SG100-SIL*, while the degrees of coverage, i.e., the average bonding densities of *modifier* in both the modified *SG100-C4* and *SG100-C18 matrices* are 3.9 or 3.7 μmol/m^2, respectively.

As extrinsic probe, *2,2,6,6-tetramethypiperidine-1-oxyl,* (*TEMPO*), from Sigma-Aldrich, Inc, Germany, was used by dissolving it in the liquid *CHX* at a very low concentration of $5x10^{-4}$ M.

A series of the confined *spin systems* for ESR studies was prepared by drop-by-drop filling of a solution of the *CHX* doped with the spin probe *TEMPO* into the *accessible* pores of all the four *SG matrices* to achieve a completely filled (saturated) state of the *filler* (*CHX*) in the pores of the *confiners* (*SG's*). The capillary forces allowed to fill the *accessible* pores of *SG* with *CHX* with no liquid remainders on the external surface *of the SG* grains. The *theoretical* and *real* mass fractions of the *filler* for the each *filler/confiner system,* as well as the ratio of the latter quantity to the former one are given in Table 1. Before the own filling procedure all the four *SG matrices* were dried at 393 K for several hours, to evaporate the adsorbed *water*.

2.2. DSC

DSC measurements were carried out on DSC 8500 from Perkin-Elmer based on a power compensation principle equipped with a CLN2 cooler. Calibration was performed with a series of three different standard substances: *indium, n-dodecane* and *n-heptane*. The sample masses were about 15 mg. All DSC measurements were carried out under nitrogen atmosphere using standard aluminium pans. The samples were first cooled with −10 K/min from room temperature down to 113 K and subsequently, they were measured with heating rate of + 10 K/min from 113 K up to 303 K. The *solid*-to-*solid* and *solid*-to-*liquid* (melting) transition phenomena, i.e., endothermal effects in the DSC thermogram, were quantified by the onset *solid*-to-*solid* transformation temperatures, $T_{ss}(D_{pore})$, and the onset melting transition temperatures, $T_m(D_{pore})$, and the corresponding *solid*-to-*solid* transformation enthalpy, $\Delta H_m(D_{pore})$, and *melting* transition enthalpy, $\Delta H_m(D_{pore})$, were normalized to the mass of *CHX*.

2.3. ESR

ESR measurements of the spin systems *TEMPO/CHX* were performed with the X-band Bruker – ER 200 SRL spectrometer operating at 9.4 GHz with a Bruker BVT 100 temperature variation controller unit. ESR spectra of the doped *TEMPO/CHX systems* were slowly cooled with ca. −4 K/min rate and subsequently were recorded in heating mode

Table 1
Physical parameters of a series of the used *SG matrices* according to the *supplier* and the confined *CHX/SG* systems.

Matrix	Pore diameter D_{pore}, Å	Pore size distribution %	Pore volume V_{pore}, cm^3/g	Pore area A_{pore}, m^2/g	$F_{CHX,theo}$* –	$F_{CHX,sat}$** –	%***
SG 60-SIL	60	80 ± 15	1.20	546	0.483	0.479	99.1
SG 100-SIL	100	80 ± 25	0.85	312	0.398	0.381	96
SG 100-C4			0.92	327	0.417	0.399	95.7
SG 100-C18						0.298	
SG 300-SIL	300	80 ± 25	0.93	112	0.420	0.411	97.8

* $F_{CHX,theo} = m_{CHX}/(m_{CHX} + m_{SG})$, the theoretical mass fraction of *CHX medium* with respect to the *CHX/SG system* estimated using the density of *CHX* at room temperature, $\rho_{CHX}(RT) = 0.779\ g/cm^3$ under the complete accessibility condition of all the pores for the *CHX medium*.

** $F_{CHX,sat} = m_{CHX}/(m_{CHX} + m_{SG})$, the real experimental mass fraction of *CHX* in the *CHX/SG system* corresponding to the fully filled (saturated) situation of the *CHX* in the *CHX/SG system*.

*** $\% = F_{CHX,sat}/F_{CHX,theo} \times 100$.

over a wide temperature range from 115 K up to 350 K using temperature steps of 5–10 K. To reach thermal equilibrium, the samples were kept at a given temperature for 15 min before the starting of the spectra accumulations. In these measurement the temperature stability was ± 0.5 K. The microwave power and the amplitude of the field modulation were optimized to avoid signal distortion. Analysis of the ESR spectra was performed in terms of the extrema separation of the outermost lines of the triplet spectra, $2A_{zz'}$, as a function of temperature with subsequent evaluation of the spectral parameter of mobility T_{50G} [11,13] as well as further characteristic ESR temperatures, T_{Xi}, within both slow and fast motional regimes: T_{Xi}^{slow}, T_{Xi}^{fast} [14,23].

3. Results and discussion

3.1. DSC data

The macroscopic structural-phase-transition temperatures characterization of bulk *CHX medium* as well as of a series of the confined *CHX/SG samples* were characterized by means of DSC are summarized in Fig. 1 and Table 2.

The obtained thermodynamic data of both the phase transitions in the bulk *CHX* are in a plausible agreement with those from the literature: $T_m = 280.1$ K [26], $T_{ss} = 186$ K, $T_m = 281$ K, $\Delta H_{ss} = 79.8$ J/g and $\Delta H_m = 31.9$ J/g [27] and $T_m = 279.5$ K, $\Delta H_m = 31.3$ J/g [41]. On the other hand, the DSC characteristics of the *CHX* after insertion of the organic *filler* into the various inorganic *SG confiners* behave in different way depending on the quality of the pores surface. It is therefore usefull to divide and discuss these changes according the two types of surface composition of the used *SG matrices*.

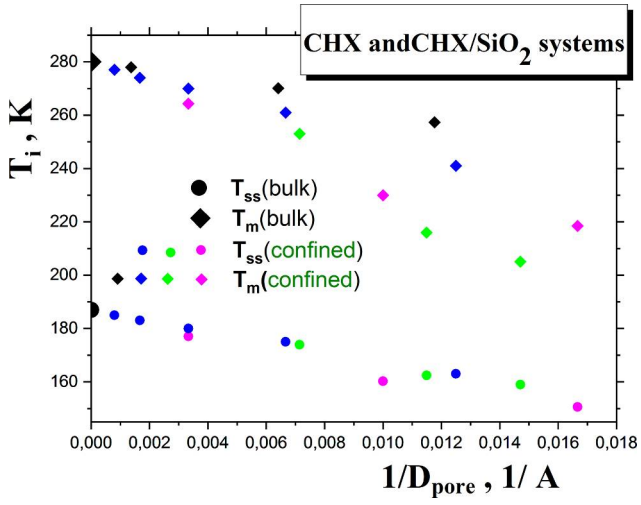

Fig. 1. Phase i.e. *solid*-to-*solid*, T_{ss}, (circles) and *solid*-to-*liquid* (melting), T_m, (diamonds) transformation temperatures as a function of inverse pore diameter, $1/D_{pore}$ for *CHX* confined in irregular modified *CPG matrices* [26] (black points), irregular modified *silica gel matrices* [27] (blue points), in regular unmodified *SBA-15 matrices* [33,42] (green points) and irregular unmodified *silica gels SG–SIL matrices* [present work] (magenta points). Initial larger circle and diamond mark T_{ss} or T_m of the bulk *CHX* with $1/D_{pore} = \infty$, respectively. (For interpretation of the references to colour in this figure legend, the reader is referred to the web version of this article.)

First, in the series of the three virgin *SG300-SIL, SG100-SIL* and *SG60-SIL matrices,* both the phase transiton temperatures T_{ss} and T_m are decreased significantly with physical restriction, i.e., with the decrease of the mean pore diameter D_{pore} from 300 Å through 100 Å down to 60 Å. For the largest spatial limitation these reductions in the T_{ss} and T_m values reach −36.4 K or −61.5 K, respectively. Similarly, the dramatic reductions in the phase transformation enthalpies ΔH_{ss} and ΔH_m occur as they will be presented and discussed later. All these changes in the thermodynamic characteristics on confinement of the *CHX medium* reflect its significant structural-phase reorganization towards the increased rotation disorder in the *solid* state as well as the elevated amorphization of the *CHX medium* after its spatial restriction into the mesopores of the virgin *SG-SIL matrices* with respect to the highly rotation and translation ordered (crystalline) structure of *CHX* in the bulk state.

It is of interest to compare the present DSC data on three virgin *silica gels* with previous data for both the phase transitions of variously confined *CHX* in the literature [26,27,33]. Fig. 1 shows such a comparison with sets of data on three irregular *controlled porous glasses* (*CPG*) *matrices* modified by silylation with *hexamethyldisilazane* giving very short $\equiv Si{-}O{-}Si(CH_3)_3$ grafts instead of the original *silanol* groups [26]. Furthermore, it provides T_{ss} and T_m of the five irregular *silica* (*Spherosil*) *matrices* modified by dehydratation and dehydroxylation [27] as well as on the three regular unmodified *SBA-15 matrices* [33,42]. As one can see, in the case the *solid*-to-*solid* transition the T_{ss} data are quite close to each other with sligthly larger difference for the irregular unmodified *SG-SIL matrices* indicating a rather weak

Table 2
Temperature and enthalpy of *solid*-to-*solid* (T_{ss}^{DSC}, (ΔH_{ss}^{DSC}) and *solid*-to-*liquid* (melting) (T_m^{DSC}, ΔH_m^{DSC}) phase transformations and temperature differences $\Delta T_i = T_i(conf) - T_i$ (bulk), where $T_i = T_{ss}^{DSC}$ or T_m^{DSC} in the bulk *CHX* and a series of the various confined *CHX/SG systems*. Typical temperature and enthalpy uncertainties are up to ± 1 K and ± 1.5 J/g.

Sample	T_{ss}^{DSC} K	ΔT_{ss} K	ΔH_{ss} J/g *CHX*	T_m^{DSC} K	ΔT_m K	ΔH_m J/g *CHX*
CHX	187	0	78.5	280	0	32
CHX/SG300Å	177	−10	22.2	264.3	−15.7	7.2
CHX/SG100Å	160.2	−26.8	20.5	230	−50	2.8
CHX/SG100Å-***C4***	162.2	−24.8	21	234	−46	9.4
CHX/SG100Å-***C18***	145	−42	8.3	225	−55	10.5
CHX/SG60Å	150.6	−36.4	19.7	218.5	−61.5	4

sensitivity to the type of the confining SiO_2–based *matrix*, perhaps. On the other hand, as for T_m, in addition to the generally larger depression of the *melting* transition temperature, we find a rather larger dependence on the type of SiO_2-based *matrix*. Moreover, the T_m values seem to group roughly into two classes reflecting the effect of surface composition on the T_m reduction, being weaker for hydrophobic walls of the pores in the modified *CPG*'s and *SG*'s than for the hydrophilic ones in the unmodified *SBA-15* and our series of unmodified (virgin) *SG-SIL matrices*. These findings suggest a complex picture for the confined *CHX* in various SiO_2-based *confiners*. While the former transition is related to a *smaller*-scale rearangement connected with the rotational disordering of the *CHX* molecules and is only weakly dependent on the pore morphology and chemistry, the latter case is related to a *large*-scale phase transition due to translational disordering and depends sensivitely on various aspects of the pore morphology and chemistry, e.g. not only on pore regularity or irregularity,i.e., pore separability or pore interconnectivity, but also on pore sizes distribution as well as pore surface composition.

In addition, the effect of pore surface modification on the DSC characteristics can be evaluated in detail for the two modified *SG100 matrices*. One modification included replacement of a part of the original *polar silanol* $\equiv SiOH$ groups by *apolar* ones, such as the shorter *dimethylbutylsilyl* groups $\equiv Si{-}O{-}Si(CH_3)_2(CH_2)_3CH_3$ in *SG100-C4 matrix* and the other one by the essentially longer *dimethyloctadecylsilyl* groups $\equiv Si{-}O{-}Si(CH_3)_2(CH_2)_{17}CH_3$ in *SG100-C18*. In the former case of shorter grafts one observes the slight increase of T_{ss} and T_m by ca. +2 or +4 K, respectively, compared to the virgin *SG100-SIL matrix*. On the other hand, in the case of the significantly (more than 4 times) longer grafts in the *SG100-C18*, larger reductions of T_{ss} by about −42 K and of T_m by about −55 K with respect to the bulk *CHX* is found. Interestingly, the latter decrease of T_m is a bit about −5 K larger than the one for the virgin *SG 100-SIL matrix*. At first sight we could expect a further reduction in both the T_{ss} and T_m values with respect to the virgin *SG100-SIL matrix* due to the smaller effective pore size, but the situation is not so simple.

In the literature one similar DSC study on the *CHX* in the *SG80 matrix* modified via dehydratation and dehydroxylation treament and in the two chemically-derivatized *SG80-C1* (*trimethylsilyl,* $-O{-}Si(CH_3)_3$) and *SG80-C6* (*hexyl*,$-O{-}(CH_2)_5CH_3$) *matrices* exists [28]. It was found that the differences in the melting temperature ΔT_m, defined as T_m(conf)–T_m(bulk) reach −27 K, −44 K and −31 K. These authors concluded that the observed non-monotonous trend in the melting temperature with the alkyl modifier length cannot simply be attributed only to the "shrinkage" of the pore size due to the presence of the short $-O{-}Si(CH_3)_3$, or the longer $-O{-}(CH_2)_5CH_3$ groups on the *silica gel* surface wall as in the case of the aliphatic linear *n-alkane*, i.e., *n-decane*, where this intuitive supposition is found to be valid [28].

Our data on the modified *SG100-C4* and *SG100-C18 matrices* seem to exhibit similar non-monotonous order of $\Delta T_m = -50$ K, −45 K and −55 K as a function of the modifying *alkylsilyl* group length in the *SG100-SIL, SG100-C4* and *SG100-C18 matrices,* at first sight, with the rather, unexpected smaller reduction $\Delta T_m = -55$ K for the *CHX/SG100-C18 system* compared with the virgin *SG60-SIL* with $\Delta T_m = -61.5$ K. According to the detailed experimental and modelling study of the geometry of the pores in a series of empty modified *SG's*, the effective pore size is not given simply by the *linear* correction of the original pore diameter on the straight alkylsilyl modifier length because of its coiled minimized-energy conformation [43,44]. However, the situation is complicated in the presence of the confined *organic medium* in the *modified confiner* due to the possibility that the conformation of longer alkyl modifier may further be altered with respect to that in the empty *SG matrix*. Consequently, the observed trend results also from additional interaction between the *apolar* alkyl modifier and *apolar CHX medium* in the confined state by the modified *confiner*.

As for the energetic aspect of phase transitions, the *solid*-to-*solid* transformation enthalpy, ΔH_{ss}, and the *solid*-to-*liquid* (melting) transition enthalpy, ΔH_m, also decrease drastically in accord with the literature [26,28,29]. Thus, for the most restrictive situation in a series of the three virgin *SG-SIL matrices,* the ΔH_{ss} value is reduced by 75%, while the ΔH_m even by 87.5%. These values indicate very essential disordering and amorphization of the *CHX medium* after physical restriction.

Next, the corresponding transformation enthalpies have rather different trends. Thus, the ΔH_{ss} value is comparable for the shorter *C4 modifier* with the virgin *SG100-SIL matrix* and essentially lower for the longer *C18 alkyl group*. On the other hand, the ΔH_m increases with *alkylsilyl* chain lenght in comparison with the parent *SG100-SIL matrix*. This suggests that the orientation order of the *CHX molecules* decreases with an introduction of *alkylsilyl groups*, but in contrary, their translational order increases with respect to the rotation-translation situation in the the virgin *SG100-SIL matrix*.

All these changes in the thermodynamic characteristics indicate the essential structural-phase reorganization of the *CHX medium* towards significant amorphization after its spatial restriction into the mesopores of the virgin *SG-SIL matrices* and the modified *SG100-C4* and *SG100-C18 matrices* with respect to the highly ordered (crystalline) structure in the bulk state.

3.2. ESR data

Figs. 2 and 3 show the spectral parameter, $2A_{zz'}$, as a function of temperature for all the six investigated *CHX* systems. For the sake of clearness, the ESR data and their discussions are separated into two groups in dependence on the chemical composition of the pore surface of the *SG confiners*.

3.2.1. ESR data for CHX confined in the unmodified (virgin) SG-SIL matrices

Basically quasi-sigmoidal, significantly distinct $2A_{zz'}$ vs. *T* plots depending on the physical, i.e. bulk or confined state of the *CHX medium* as well as on the pore size of the virgin *SG matrices* are found in Fig. 2. In the bulk *CHX medium,* the $2A_{zz'}$ values at the lowest temperature of our measurements reach from 67 Gauss to ca. 32 Gauss at *RT*, being

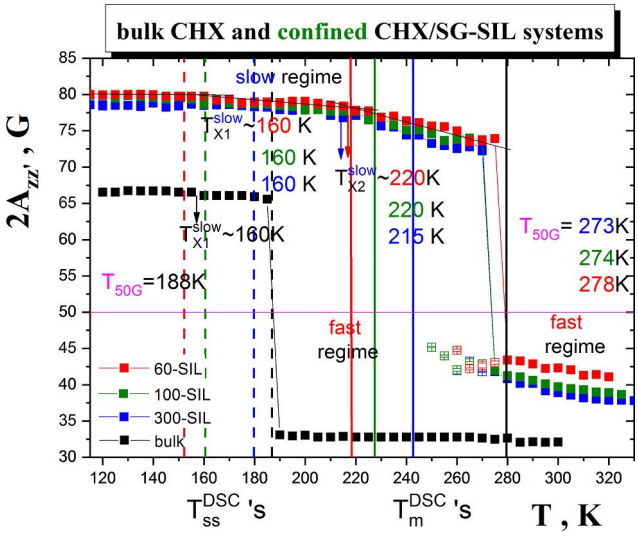

Fig. 2. Spectral parameter $2A_{zz'}$ of the spin probe *TEMPO* as a function of temperature in the bulk *CHX* and the three confined *CHX/SG 60, 100* and *300-SIL* systems demonstrating the effect of pore size D_{pore} in the unmodified *SG-SIL matrices.* The characteristic ESR temperatures T_{X1}^{slow}, T_{50G} and T_{X1}^{fast} for the bulk CHX and T_{X1}^{slow}, T_{X2}^{slow} and T_{50G} for the confined *CHX/SG 60,100* and *300-SIL systems* are marked by arrows. The characteristic DSC temperatures of both the phase transitions are also depicted by dashed lines for the *solid*-to-*solid* transitions at T_{ss} and by full lines for the melting tranformations at T_m.

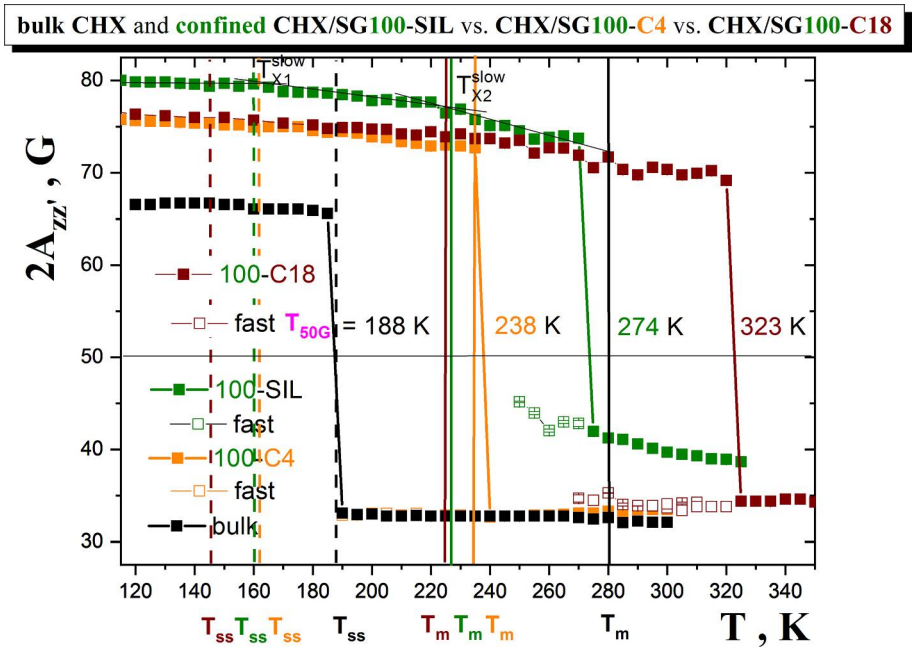

Fig. 3. Spectral parameter $2A_{zz'}$ of the spin probe *TEMPO* as a function of temperature in the bulk *CHX* and the three confined *CHX/SG100-SIL*, *CHX/SG100-C4* and *CHX/SG100-C18* systems demonstrating the dramatic effect of the pore wall composition in the modified *SG100-CX matrices.*

typical for *nitroxide free radicals* in *apolar* organic *media* [45–49]. The most pronounced change at the characteristic ESR temperature T_{50G} correlates with T_{ss} [40]. In addition, two weak changes in $2A_{zz'}$ can be found, one within the slow motion regime at $T_{X1}^{slow} \sim 160$ K and the other within the fast one at $T_{X1}^{fast} \sim 280$ K, the latter being related with the *solid*-to-*liquid* transition at the melting point T_m(*bulk*).

Confinement of the spin probe *TEMPO* doped *CHX medium* in a series of three virgin *SG-SIL matrices* lead to very significant changes in both the $2A_{zz'}$ value at 115 K and 300 K as well as in the characteristic ESR temperatures, T_{Xi}^{slow} and T_{50G} which mark numerous changes in the temperature dependencies.

As for the values of $2A_{zz'}$(115 K), the drastic increase from 67 Gauss to about 80 Gauss in the immobilized state of the *spin probe TEMPO* in all the three confined *CHX/SG-SIL systems* is found. It indicates a strong change in the mutual interaction between the *polar TEMPO* molecules and the *polar* component of the confined *CHX/SG-SILsystem*, i.e., the virgin *SG-SIL matrices* compared to their relative weak interaction with the *CHX medium* alone. Consistently, the $2A_{zz'}$(300 K) values of *TEMPO* in the confined states ranging from 38 up to 43 Gauss in all the three *CHX/SG-SIL systems* are also significantly higher compared to ca. 32 Gauss for *TEMPO* in the *bulk CHX medium* in consistency with the literature data on the adsorbed *nitroxides* on pure *silica* [24].

On increasing temperature, the three confined *CHX/SG60-SIL, CHX/SG100-SIL* and *CHX/SG300-SIL systems* reveal the first weak anomalies in $2A_{zz'}$ close to $T_{X1}^{slow} \sim 150$–160 K, in the vicinity of the reduced T_{ss}(confined) transitions.

On further increase the temperature, the second stronger changes in $2A_{zz'}$ are shifted from $T_{X1}^{slow} \sim 160$ K in the bulk *CHX* to T_{X2}^{slow}(confined) ~ 215, 220 and 220 K for the virgin *SG300-SIL*, *SG100-SIL* and *SG60-SIL matrices*. Further enhancement of the temperature leads to the most pronounced transition from the slow to the fast motion regime that occur at T_{50G} = 273, 274 and 278 K, respectively. Comparison of the characteristic ESR temperatures T_{X1}^{slow} and T_{50G} with those of the phase transitions reveals a correlation of T_{X1}^{slow}(confined) with the decreased melting temperature for the smallest pores T_m(60 Å) indicating a sensitivity of the surface-bonded reorienting *TEMPO probe* dynamics to the phase transition for the maximal confinement of the *CHX/SG60-SIL system*. On the other hand, the effect of the phase transition for the 100 Å and 300 Å restrictions is not so apparent suggesting the local character of the change within the slow motion regime. Finally, the most pronounced slow to fast motion transitions lie essentially above the corresponding T_m(confined), but in the relative vicinity also supporting the local character of the phenomenon. Interestingly, the T_{50G} values for our set of the confined *CHX/SG60-SIL, 100-SIL* and *300-SIL systems* are about 25 K below those for another *apolar organics*, i.e., linear *n-alkanes*, such as *n-hexadecane* (*n-HXD*) in the same series of the virgin *SG-SIL confiners* [14] with T_{50G} = 298–313 K and *n-undecane* (*n-UND*) [49] in the same virgin *SG100-SIL* with T_{50G} = 298 K. This finding seems to indicate that for the *apolar* aliphatic organic *media* the T_{50G} value is somewhat dependent on the *cyclic* vs. *acyclic* topology of the *molecular constituents.*

3.2.2. ESR data for CHX confined in the modified SG100-C4 and SG100-C18 matrices

Similarly as in the previous case, basically quasi-sigmoidal, significantly distinct $2A_{zz'}$ vs. *T* plots depending not only on the physical, i.e., bulk vs. confined, state of the *CHX medium,* but also on the pore surface composition of the *SG100 matrices* are observed. Thus, the $2A_{zz'}$(115 K) values for both the modified *SG100 confiners* lie in between those for the bulk *CHX medium,* i.e., 67 Gauss, and the virgin *CHX/SG100-SIL matrix*, i.e. ~80 Gauss, while for the *SG100-C4 confiner* is a bit smaller than for the *SG100-C18* one: 76 < 77 Gauss. The fact that both the $2A_{zz'}$(115 K) values do not reach the maximal $2A_{zz'}$(115 K) ~80 Gauss, being attributed to the *TEMPO* molecules attached to the pore wall, indicates that the *TEMPO probe* reflects the structural-dynamic changes of the various confined *CHX medium systems*.

In the modified *SG100-C4 matrix* with the shorter *alkyl silyl* groups, the slow to fast transition with respect to the virgin *SG100–SIL matrix* with T_{50G} = 274 K is shifted by 36 K to the lower temperature of T_{50G} = 238 K. On the other hand, the other modified *SG100-C18 matrix* with essentially longer *alkyl silyl* groups causes a slowing down of the slow to fast transition at the T_{50G} = 323 K compared to the the virgin *SG100–SIL matrix*. These mutual relationships between all the three types of *SG100 matrices* can be explained by considering the following two factors: effective pore size and pore surface composition.

Regarding the first factor, the effective pore size is reduced after any chemical modification by adding the alkyl groups [43,44]. It might imply that the dynamics should be slowed down with respect to that in

the *virgin SG100-SIL matrix*. Indeed, although this is found for the *SG100-C18* case, for the shorter modifier in the *SG100-C4 matrix* the opposite situation exists. According to the detailed experimental and modelling study of the geometry of the pores in a series of empty modified *SG's*, the effective pore size is not given simply by the *linear* correction of the original pore diameter on the straight alkylsilyl *modifier* length because of its *coiled* energy-minimized conformation [43,44]. However, in the presence of the confined organic *medium* in the *modified confiner*, the real conformation situation of the *modifier* might be complicated by the possibility that the conformation of longer alkyl silyl *modifier* can further be altered with respect to that in the empty *SG matrix*. Consequently, the observed trend results also from certain additional interaction between the *apolar alkylsilyl modifier* and *apolar CHX medium* in the confined state.

As for the second aspect, we recall that the average bonding density of *modifier* in both the modified *SG100 matrices* are quite close being 3.9 μmol/m^2 or 3.7 μmol/m^2, respectively. This means that about 48.8% or 46.3% of the total surface concentration of the original *silanol* groups 8 μmol/m^2 are substituted by the corresponding *modifier* indicating an almost comparable degree of coverage of the pore surface by the *alkylsilyl* groups. Evidently, the complete substitution of all the *silanol* groups at the original pore surface for the sterical reasons is impossible. Both the *alkylsilyl* groups *C4* and *C18* increase the hydrophobic character of the pores and this coverage of the pore surface decreases an approach of the *TEMPO probes* to the remaining unreacted *silanol* groups. Thus, they reduce the potential interaction the *polar spin probe TEMPO molecules* with them. However, the shorter *alkylsilyl* groups of *modifier* reduce the effective pore volume to an essentially smaller extent and this fact together with the similar coverage of the pore surface by *apolar dimethylbutylsilyl* groups results globally in a decrease of the T_{50G} value with respect to the virgin *CHX/SG100-SIL* case, i.e., an acceleration of the transition from slow to fast motion regime. On the other hand, although the longer and coiled *C18* groups [43] seem to change the pore surface to the hydrophobic character to an essentially larger extent with better coverage of the remaining unreacted *silanol* groups, the smaller effective pore diameter together with the larger probability of the presence of a certain fraction of the *CHX* molecules as well as the *TEMPO ones* in between the longer *modifier chains* leads effectively to the dominance of the latter aspect. As the result, the significant increase in the T_{50G} value with respect to the *virgin SG100-SIL matrix*. Evidently, in this case of *CHX/SG100-C18 system* ESR technique measures and reflect rather the *qualitatively* different confined *system* compared to the *CHX/SG100-C4* and *CHX/SG100-SIL ones.*

4. Conclusions

The spectral behavior of the spin probe *TEMPO* in the bulk cyclic hydrocarbon *cyclohexane* (*CHX*) and its confined states in a series of *silica gels* (*SG*) and phase behavior using ESR or DSC, respectively, are reported. The spectral parameter $A_{zz'}$ at low and high temperatures and the characteristic ESR temperature T_{50G} of the slow to fast regime transition of *TEMPO* increases dramatically in the virgin *SG-SIL*'s compared to the bulk *CHX medium* weakly depending on the pores size. This trend is similar to that found for other linear hydrocarbon, *n-hexadecane* (*n-HXD*). In contrast, the sensitivity to the pores size for the globular *CHX* molecules is slighter in comparison to the moderate one for the linear *n-HXD* molecules. On the other side, the $A_{zz'}$ values and the corresponding T_{50G} ones are very dependent on the pores composition confirming definitely the hypothesis about the preferential localization of polar *molecular probe* to polar pores of the *SG matrices*. These observations result from the complex interrelation between the mutual interaction between the polar *TEMPO* and the polar or apolar *SG*'s and the altered phase behavior of the *CHX* as evidenced from DSC. These findings point to very careful choice of the organic *filler* and inorganic *confiner* in the bulk vs. confinement problem as monitored not only by ESR technique but also by other molecular probes, such as fluorescence ones. The results of further investigations for organic *medium* of distinct structural type, such as polar protic substance, inserted in the same series of inorganic *SG matrices* which allowing for its preferential interaction with their pores over that with the *polar spin probe* will be presented elsewhere.

Declaration of Competing Interest

The authors declare that they have no known competing financial interests or personal relationships that could have appeared to influence the work reported in this paper.

Acknowledgements

This work was supported by the Slovak Research and Development Agency (SRDA) under the contract No. APVV-16-0369. We also thank the VEGA Agency, Slovakia for Grant No. 2/0030/16 and the Croatian Science Foundation (project 3168).

References

[1] S. Napolitano, E. Glynos, N.B. Tito, Glass transition of polymers in bulk, confined geometries and near interfaces, Rep. Prog. Phys. 80 (2017) 036602.
[2] P. Huber, Soft matter in hard confinement: phase transition thermodynamics, structure, texture, diffusion and flow in nanoporous media, J. Phys.: Condens. Matter 27 (2015) 103102.
[3] C. Alba-Simionesco, B. Coasne, G. Dosseh, G. Dudziak, K.E. Gubbins, R. Radhakrishnan, M. Sliwinska-Bartkowiak, Effects of confinement on freezing and melting, J. Phys.: Condens. Matter 18 (2006) R15.
[4] M. Alcoutlabi, G.B. McKenna, Effects of confinement on material behavior at the nanometre size scale, J. Phys.: Condens. Matter 17 (2005) R461.
[5] F. Kremer (Ed.), Dynamics in Geometrical Confinement, Springer, Heidelbeg, 2014.
[6] R. Richert, Dynamics of nanoconfined supercooled liquids, Annu. Rev. Phys. Chem. 62 (2011) 65.
[7] A. Schönhals, R. Zorn, B. Frick, Inelastic neutron scattering as a tool to investigate nanoconfined polymer systems, Polymer 105 (2016) 393.
[8] M. Kruteva, A. Wischnevski, D. Richter, Polymer dynamics in nanoconfinement: interfaces and interphases, Eur. Phys. J. Conf. 83 (2015) 02009.
[9] S.N. Bhat, A. Sharma, S.V. Bhat, Vitrification and glass transition of water: insight from spin probe ESR, Phys. Rev. Letts. 95 (2005) 235702.
[10] R. Owenius, M. Engström, M. Lindgren, Influence of solvent polarity and hydrogen bonding on the EPR parameters of a nitroxide spin label studied by 9-GHz and 95-GHz EPR spectroscopy and DFT calculation, J. Phys. Chem. A 105 (2001) 10967.
[11] G.G. Cameron, Comprehensive Polymer Science, Pergamon Press, Oxford, 1989, p. 517.
[12] M. Veksli, M. Andreis, B. Rakvin, ESR spectroscopy for the study of polymer heterogeneity, Prog. Polym. Sci. 25 (2000) 949.
[13] G.P. Rabold, Spin probe studies. II. Application to polymer characterization, J. Polym. Sci. A 17 (1969) 1203.
[14] M. Lukešová, H. Švajdlenková, P. Sippel, E. Macová, D. Berek, A. Loidl, J. Bartoš, Spin probe dynamics of n-hexadecane in confined geometry, Eur. Phys. J. B 88 (2015) 46.
[15] S. Anandan, M. Okazaki, Dynamics, flow motion and nanopore effects of molecules present in the MCM-41 Nanopores, Micro- Mesopor. Mater. 87 (2005) 77.
[16] G. Martini, Water and other polar liquids in porous systems studied by ESR and ESE, Coll. Surf. 45 (1990) 83.
[17] G. Martini, M.F. Ottaviani, M. Romanelli, L. Kevan, ESR in surface science, Coll. Surf. 41 (1989) 149.
[18] H. Yoshioka, Phase transition of the water confined in porous glass as studied by the spin probe method, J. Chem. Phys. Soc.-Faraday Trans. 84 (1988) 4509.
[19] M. Roussenova, M.A. Alam, S. Townrow, D. Kilburn, P.E. Sokol, R. Guillet-Nicolas, F. Kleitz, A nano-scale free volume perspective on the glass transition of supercooled water in confinement, New J. of Physics 16 (2014) 103030.
[20] R. Zaleski, T. Goworek, n-Nonadecane embedded in mesopores, Mat. Sci. Forum 607 (2009) 180.
[21] M. Iskrová, V. Majerník, E. Illeková, O. Šauša, D. Berek, J. Krištiak, Free volume seen by positronium in bulk and confined molecular liquid, Mat. Sci. Forum 607 (2009) 235.
[22] D. Dutta, P.K. Pujari, K. Sudarshan, S.K. Sharma, Effect of confinement on the phase transition of benzene in nanoporous silica: a positron annihilation study, J. Phys. Chem. C 112 (2008) 19055.
[23] J. Bartoš, H. Švajdlenková, R. Zaleski, M. Edelmann, M. Lukešová, Spin probe dynamics in relation to free volume in crystalline oreganics by ESR and PALS: n-Hexadecane, Physica B 430 (2013) 99.
[24] G.P. Lozos, B.M. Hoffman, Electron paramagnetic resonance of adsorbed nitroxide, J. Phys. Chem. 78 (1974) 200.
[25] J. Tiňo, P. Mach, Z. Hloušková, I. Chodák, Restriction of spin probe motion in polymer composites due to chemical factors, J. Macromol. Chem. Pure Appl. Chem.

A 31 (1994) 1481.
[26] C.L. Jackson, G.B. McKenna, The melting behavior of organic materials in porous solids, J. Chem. Phys. 93 (1990) 9002.
[27] V. Mu, V.M. Malhotra, Effect of surface and physical confinement on the phase transition of cyclohexane in porous Silica, Phys. Rev. B 44 (1991) 4292.
[28] V.M. Malhotra, R. Mu, A. Natarajan, Effects of surfaces on the melting/freezing behavior of fluids in derivatized- and nude-porous silica, MRS Symp. Proc. 290 (1993) 121.
[29] S. Amanuel, V.M. Malhotra, Comparative thermodynamic behavior of physically restricted cyclohexane in porous silica, MRS Symp. Proc. 543 (1998) 45.
[30] S. Amanuel, H. Bauer, P. Bonventre, D. Lasher, Nonfreezing interfacial layers of cyclohexane in nanoporous silica, J. Phys. Chem. C 113 (2009) 18 983.
[31] C. Faivre, D. Belleta, G. Dolino, Phase transitions of fluids confined in porous silicon: a differential calorimetry investigation, Eur. Phys. J. B 7 (1999) 19.
[32] D. Morineau, G. Dosseh, C. Alba-Simionesco, P. Llewellyn, Glass transition, freezing and melting of liquids confined in the mesoporous silicate MCM-41, Phil. Mag. B 79 (1999) 1847.
[33] G. Dosseh, Y. Xia, C. Alba-Simionesco, Cyclohexane and benzene confined in MCM-41 and SBA-15: confinement effects on freezing and melting, J. Phys. Chem. B 107 (2003) 6445.
[34] J.C. Dore, M. Dunn, T. Hasebe, J.H. Strange, Orientationally disoredered crystals in porous silica: cyclohexane, Coll. Surf. 36 (1989) 199.
[35] H. Farman, J.C. Dore, J.B.W. Webber, Some unusual features in the behavior of cyclohexane in confined geometry studied by neutron scattering, J. Mol. Liquids 96–97 (2002) 353.
[36] H.F. Booth, J.H. Strange, Organic nanocrystals: an NMR study of cyclohexane in porous silica, Mol. Phys. 92 (1998) 263.
[37] J.H. Strange, H. Rahman, Characterization of porous solids by NMR, Phys. Rev. Letts. 71 (1993) 3589.
[38] D.W. Aksnes, L. Gjerdaker, NMR line width, relaxation and diffusion studies of cyclohexane confined in porous silica, J. Mol. Struct. 475 (1999) 27.
[39] L. Gjerdaker, D.W. Aksnes, G.H. Sorland, M. Stoecker, Relaxation and diffusion studies of cyclohexane confined in MCM-41 by NMR, Micropor. Mesopor. Mater. 42 (2001) 89.
[40] H. Švajdlenková, B. Zgardzinska, M. Lukešová, J. Bartoš, Spin probe dynamics in relation to free volume in crystalline organics from ESR and PALS: cyclohexane, Chem. Phys. Letts. 643 (2016) 98.
[41] R.C. Weast (Ed.), Handbook of Chemistry and Physics, 56th ed., Chemical Rubber Co., Cleveland, 1975.
[42] Note about the error in the pore size quantification in Table 3 and Figs. 10 and 12 in Ref. 33; the pore sizes are given as the pore diameter instead of the pore radius – see the original Ref. 27.
[43] I. Rustamov, T. Farcas, F. Ahmed, F. Chan, R. LoBrutto, H.M. McNair, Y.V. Kazakevic, Geometry of chemically modified silica, J. Chrom. A 913 (2001) 49.
[44] O. Šauša, J. Krištiak, D. Berek, M. Iskrová, Column packing for high-performance liquid chromatography and positron annihilation spectroscopy, Rad. Phys. Chem. 76 (2007) 271.
[45] P. Mukerjee, C. Ramachandran, R.A. Pyter, Solvent effects on the visible spectra of nitroxides and relation to nitrogen hyperfine splitting constants. Nonempirical polarity scales for aprotic and hydroxylic solvents, J. Phys. Chem. 86 (1982) 3189.
[46] B.R. Knauer, J.J. Napier, The hydrogen hyperfine splitting constant of the nitroxide functional group as a solvent polarity parameter, J. Amer. Chem. Soc. 98 (1976) 4395.
[47] O.H. Griffith, P.J. Dehlinger, S.P. Van, Shape of the hydrophobic barrier of phospholipid bilayers, J. Membr. Biol. 15 (1974) 159.
[48] Y. Murata, N. Mataga, ESR and optical studies on the EDA complexes of di-t-butylnitroxide radical, Bull. Chem. Soc. Japan 44 (1971) 354.
[49] J. Bartoš, O. Šauša, H. Švajdlenková, I. Matko, K. Čechová, Bulk and confined n - alkanes: n - undecane in unmodified vs. modified silica gels by positron annihilation lifetime spectroscopy and electron spin resonance techniques, J. Non-Cryst. Solids 511 (2019) 1.